# Magnetostatic Modes in Highly Polarized Solid Helium-Three

D. D. Osheroff
*AT&T Bell Laboratories, Murray Hill, New Jersey 07974*

and

M. C. Cross
*Division of Physics, Mathematics, and Astronomy, California Institute of Technology, Pasadena California 91125*
(Received 1 May 1987)

We report the observation of an unusual series of spin-wave modes seen in continuous-wave NMR measurements on long cylindrical crystals of highly polarized solid $^3$He. When a magnetic field and field gradient of appropriate magnitude are placed along the cylinder axis, the NMR spectrum breaks up into a series of discrete peaks whose spacing is geometric in mode number, with the spacing going to zero at an accumulation point. We show that this behavior is consistent with magnetostatic waves in the highly polarized medium.

PACS numbers: 67.80.Jd, 41.10.Dq

In NMR experiments one frequently assumes that all the spins precess independently of the dynamical behavior of their neighbors. If a magnetic field gradient is applied across the sample, NMR absorption as a function of frequency then gives information as a function of position. However, when field differences across the sample become comparable to the bulk demagnetizing fields the local-oscillator approximation is no longer valid, and indeed under certain circumstances, entirely new spin dynamical behavior can be observed. In this paper we report a striking example of such behavior in a cylinder of highly polarized solid $^3$He.

We have used a powerful demagnetization cryostat to perform continuous-wave (cw) NMR experiments on single crystals of solid $^3$He grown below 0.6 mK at melting pressures in a variable-volume sample chamber. The measurements were all obtained in a magnetic field of 0.5224 T, between 0.4 and 2 mK. Details of the apparatus and thermometry techniques are given elsewhere.[1] The solid $^3$He crystals were grown in a 1.2-mm-diameter nylon-mesh cylinder 2 cm long whose axis was oriented vertically, along the magnetic field. The 25-$\mu$m holes in the nylon mesh were sufficiently small to constrain the solid to the interior of the cylinder, but with a 25% open area, the mesh provides rapid thermal relaxation to the surrounding liquid $^3$He. At the middle of the cylinder length, a saddle NMR coil was mounted which extended 0.4 cm in the vertical direction. Crystal growth was initiated at the bottom of the cylinder with a pulse of heat, and the cell volume was decreased until the solid-liquid interface had risen to the desired position along the length of the cylinder.

In Fig. 1, a spectrum is shown of one such crystal obtained with the interface approximately 0.5 cm above the center of the NMR region, with a positive field gradient 2.3 Oe/cm in the vertical direction. The entire line shape is strongly modulated by a series of sharp resonances, whose spacing decreases to zero at an accumulation point near the low-frequency edge of the spectrum. In this figure, the bottom of the crystal is at the left, and the top at the right. Such behavior was only observed if the field gradient was positive, and if the end of the crystal was near, but not necessarily within, the NMR region. It was seen in both the paramagnetic phase and the high-field ordered phase.[2] The behavior shown did not depend upon the sense of the frequency or field sweep, nor on the magnitude of the rf level.

In Fig. 2(a) we have plotted the logarithm of the frequency shift, $\Delta\nu$, of each peak (mode) from the accumulation point versus mode number, with the highest-frequency mode being number 1. As can be seen, $\log(\Delta\nu)$ is accurately linear in the mode number for all 28 modes measured, with the period spacing between modes ranging from over 1500 Hz to under 1 Hz. The frequency of the accumulation point was taken as a

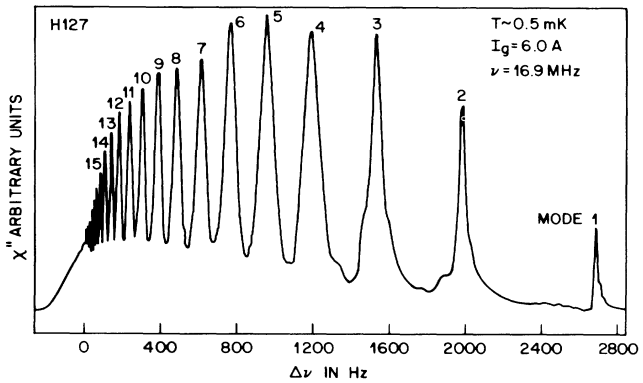


FIG. 1. Typical NMR spectrum of a cylindrical solid $^3$He crystal whose upper end is about 0.2 cm above the NMR region, and across which a positive $z$-gradient field of 1.34 Oe/cm has been applied.

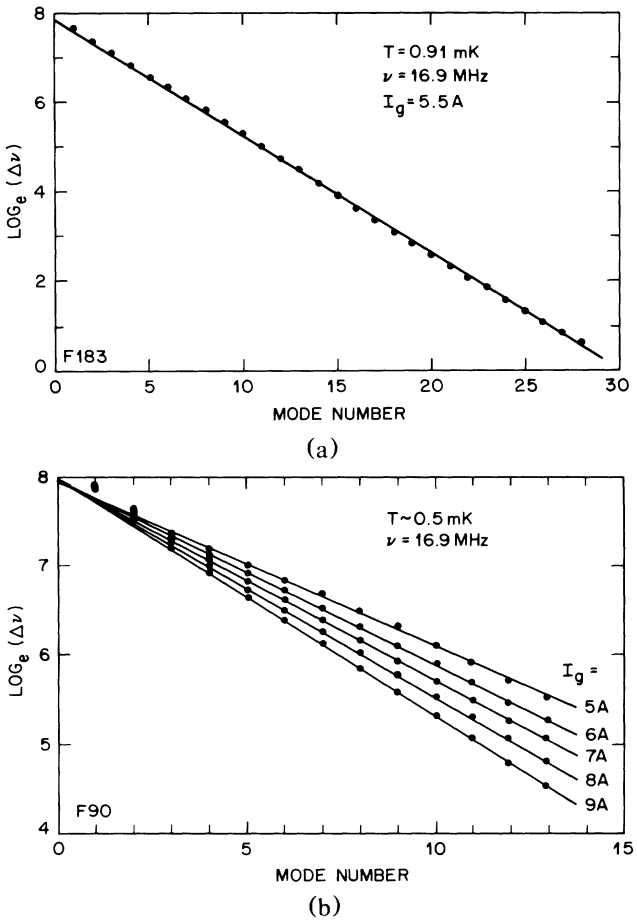


FIG. 2. (a) The exponential dependence of $\Delta\nu$, the mode frequency shift from the accumulation point, on mode number, from $\Delta\nu\simeq 1$ Hz to $\Delta\nu\simeq 2000$ Hz. (b) The dependence of $\Delta\nu$ on gradient field from 2.0 to 1.1 Oe/cm.

fitting parameter in order to make the high-$n$ portion of the curve straight, but it corresponds almost exactly with the cessation of oscillations in the spectrum.

In Fig. 2(b) we show a series of plots such as the one shown in Fig. 2(a), but here several different gradient fields have been used. Note that each straight line extrapolates to almost the same point at $n=0$, but with a different slope. Also notice that the $n=1$ point is independent of the gradient field, although well above the straight line describing the rest of the peak positions. We find that this frequency shift, $F_1$, varies by less than $\pm 1\%$ while the gradient field is varied over a factor of 2.

To test for any possible temperature dependence in the spin dynamics, we made measurements from 0.4 to 1.7 mK, spanning the magnetic phase transition in the solid at $T_c=1.02$ mK. The field gradient used was scaled with the magnetization, $M_0$, which was measured in a separate experiment and is believed accurate to $\pm 2\%$. The solid-liquid interface was adjusted at each temperature to be 0.48 cm above the center in the NMR region. If the spin dynamics is dominated by magnetostatic effects, all frequency shifts should be independent of temperature and long-range order when scaled with the magnetization. The results of this study are shown in Table I. Columns four and five show the measured frequency shifts as a fraction of the uniform demagnetizing shift, $2\pi M_0\gamma$. The absence of any significant changes in $S$, $F_0/2\pi M_0\gamma$, and $F_1/2\pi M_0\gamma$ across the nuclear ordering temperature clearly shows that the mode structure is dominated by magnetostatics, although the variation of $F_0/2\pi M_0\gamma$ with $T$ suggests that small exchange effects may also be present.

TABLE I. The temperature dependence of the spin-wave spectra scaled with the magnetization.

| $T$ (mK) | $M_0$ (cgs unit) | $S$ | $F_0/2\pi M_0\gamma$ | $F_1/2\pi M_0\gamma$ |
|---|---|---|---|---|
| 0.60 | 0.158 | 0.30 | 0.96 | 0.80 |
| 0.93 | 0.136 | 0.28 | 0.90 | 0.78 |
| 1.10 | 0.074 | 0.30 | 0.92 | 0.79 |
| 1.32 | 0.059 | 0.31 | 0.99 | 0.81 |
| 1.81 | 0.043 | 0.32 | 1.04 | 0.82 |

Finally, we have studied the dependence of $S=d\ln(\Delta\nu)/dn$ as a function of gradient field. Our best data are shown in Fig. 3, where $S^{3/2}$ is plotted versus $I_g$, the gradient current. We find that $S^{3/2}$ is accurately linear in applied gradient both for the data in Fig. 3 and the data in Fig. 2(b), and the data cannot be fitted linearly as $S^2$ vs $I_g$ or $S$ vs $I_g$. The slope of the $S^{3/2}$ vs $I_g$ curves we find vary from 0.018 to 0.015, where $dH/dz=0.223I_g$ Oe/cm.

In the following we show that this spectral behavior results from the existence of a helicoidal transverse magnetization in the sample extending from the NMR region to the upper end of the crystal, precessing at the applied frequency. There is a maximum in the local magnetic field near the upper end of the crystal produced by demagnetizing fields, and as the frequency approaches the Larmor frequency at this point from above, the pitch of the helix decreases. Each peak in Fig. 1 corresponds to the addition of one-half extra turn to the helix in the vicinity of the field maximum, and the bulk of the behavior we observe originates from spin waves trapped in a potential well surrounding this point.

Our explanation of the above behavior is based on the assumption that at each point the magnetization precesses about the local field that includes the macroscopic demagnetizing field accounting for the dipole interactions in a cubic material:

$$d\mathbf{M}/dt=\mathbf{M}\times\mathbf{H}. \quad (1)$$

Other spin-wave or exchange stiffness and damping processes are assumed negligible, but we stress that (1) does include nonlocal effects due to the dipole interactions.

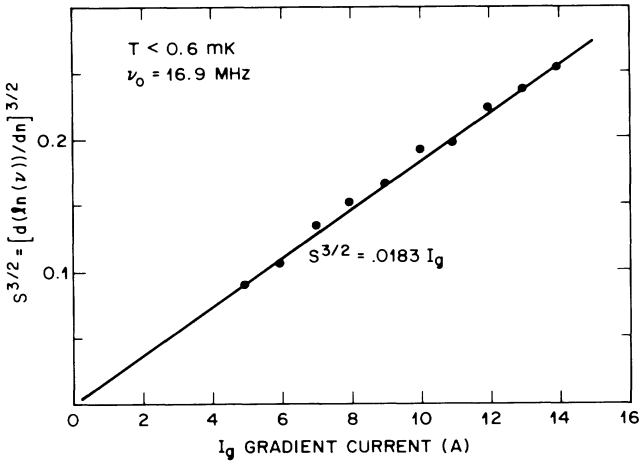


FIG. 3. The dependence of $S = d\ln(\Delta\nu)/dn$ upon gradient current. Theory predicts $S \propto (dH/dz)^{2/3}$.

The method is established by considering the simple case of a uniform external field $H_0$ along the $z$ axis of an infinite circular cylinder of magnetization $M_0$. Precession of $M_0$ about $H_0$ produces a small oscillating magnetization, $\mathbf{m}$, in the $x$-$y$ plane, and a resulting dynamic demagnetizing field $\mathbf{h}$, which reacts back on the precession, raising the resonant frequency. The field $\mathbf{h}$ can be written as an integral over surface sources $\mathbf{m}\cdot\hat{\mathbf{n}}$ with $\hat{\mathbf{n}}$ the surface normal, and volume sources $-\nabla\cdot\mathbf{m}$. This, together with (1), leads to a complicated integro-differential equation for the mode frequencies. For uniform precession, the frequency is raised by precisely $2\pi\gamma M_0$, but for large-wave-vector excitations $\mathbf{h}$ decreases and the frequency shift tends to zero. To calculate these effects we use the differential formulation introduced by Walker[3] which is particularly convenient in the limit $H_0 \gg 4\pi M_0$.[4] Then (1) may be solved (taking the positive precession frequency $\Omega$):

$$(m_x - im_y) = -M_0(h_x - ih_y)/(\Omega - H_0) \tag{2}$$

with $m_x + im_y$ negligible and setting $\gamma = 1$. We then introduce the magnetic scalar potential $\psi$ defined by $\mathbf{h} = \nabla\psi$, and use $\nabla\cdot\mathbf{b} = \nabla\cdot(\mathbf{h} + 4\pi\mathbf{m}) = 0$ to obtain an eigenvalue equation for $\Omega$:

$$-d^2\psi/dz^2 + (-\kappa)\nabla_\perp^2\psi = (-1)\nabla_\perp^2\psi \tag{3}$$

with $\kappa = -2\pi M_0/(\Omega - H_0)$. Note that except for the $\nabla_\perp^2$ operators, Eq. (3) takes the form of a Schrödinger equation.

The boundary conditions at the cylinder edge, $r = 1$, are the continuity of $\psi$ and $\mathbf{b}\cdot\hat{\mathbf{n}}$. We seek plane-wave solutions of the form $e^{ikz}e^{im\theta}F(r)$ with $k$ real. We immediately specialize to the $m = 1$ angular harmonic for $\psi$ (which corresponds to no angular dependence for $\mathbf{m}$) to insure coupling to a uniform rf magnetic field $h_1$. The boundary conditions then become the continuity of $\psi$ and $d\psi/dr + \kappa(d\psi/dr + \psi/r)$, taking $\kappa$ to be zero outside the cylinder. Then we have the following: (i) For $\kappa + 1 > 0$ (i.e., $\Omega > H_0 + 2\pi M_0$), no propagating solutions exist. The approach $\kappa \to -1^+$ is complicated, and will be discussed elsewhere. (ii) For $\Omega \to H_0$, $\kappa$ diverges to $-\infty$. The boundary condition becomes

$$d\psi/dr + \psi/r = 0, \tag{4}$$

independent of $\kappa$. The solutions to Eqs. (3) and (4) are $\psi \propto e^{ikz}e^{i\theta}J_1(\alpha_\infty r)$ with $J_0(\alpha_\infty) = 0$ and with $\Omega \to H_0 + O(1/k^2)$ as $k \to \infty$. Note that the radial structure becomes independent of $k$ in this limit, and that $\Omega$ approaches $H_0$ as $1/k^2$ as a result of a volume distribution of magnetic sources, and not exponentially as might be expected for a rapidly varying distribution of surface sources. The experimental results are essentially determined by these simple large-$k$ solutions.

We model the experiment by modifying Eqs. (1)–(4) to include $z$-dependent $H_0(z)$, $M_0(z)$, and $\kappa(z) = -2\pi M_0(z)/[\Omega - H_0(z)]$ for a static field distribution assumed uniform across the cylinder, $H_0(z) = \text{const} + gz + H_d(z)$, with $H_d(z)$ being the $z$ component of the static demagnetizing field produced by the end of the magnetized cylinder (at $z = 0$), and $g$ the applied gradient. The sharp resonance peaks are associated with the discrete modes bound in the effective potential $\kappa(z)$ for $H_{\max} < \Omega < H_{\max} + 2\pi M_0$, with $H_{\max}$ being the maximum of $H_0(z)$ at $z_{\max}$. As $\Omega \to H_{\max}$, the effective binding potential diverges, and the solution $\psi(z)$ will oscillate more and more rapidly. Each resonance observed in the experiment corresponds to an extra node of $\psi$ in this region of rapid variation for states confined in the region $H_0(z) + 2\pi M_0 > \Omega > H_0$ inside the crystal. The full structure of the solutions will be very complicated, involving a radial structure varying with $z$. However, the increasing node count approaching the accumulation point ($\Omega = H_{\max}$) is determined only by the rapid oscillations near $H_{\max}$ where $k \to \infty$. As we saw in (ii), the radial dependence separates in this limit, and we may calculate the approach to the accumulation point by solving the one-dimensional Schrödinger equation,

$$-\frac{1}{\alpha_\infty^2}\frac{d^2\psi}{dz^2} - \frac{1}{\delta_n + \Gamma^2 z^2}\psi = (-1)\psi, \tag{5}$$

for values of $\delta_n = (\Omega_n - H_{\max})/2\pi M_0$, $n$ large, such that a bound state occurs at "energy" $-1$. We have expanded $H_0(z)$ about $H_{\max}$ with $\Gamma^2 = H_0''(z_{\max})/4\pi M_0$. Since the potential and also the radial structure for large $z - z_{\max}$ are not accurately given, our solutions are only asymptotically correct as $\delta_n \to 0$. Semiclassical WKB methods[5] give $\delta_n = \exp(-Sn)$, as the experimental results suggest, with $S = \pi\Gamma/\alpha_\infty$ and $\pi/\alpha_\infty = 1.306$. To estimate $\Gamma$, we assume that $H_d(z)$ within the crystal is given by the axial field from a uniform pole density $M_0$ on the flat end of the cylindrical crystal at $z = 0$: $H_d(z) = -2\pi M_0[1 - z/(1+z^2)^{1/2}]$. For small applied gra-

dients $g$ (i.e., $g \ll 4\pi M_0$), use of the large-$z$ asymptotics of $H_d(z)$ gives $\Gamma = (\frac{3}{2})^{1/2}(g/2\pi M_0)^{2/3}$. The full expression for $H_d$ gives an answer smaller by about 10% for $I_g = 15$ A in Fig. 3. For the data shown in Fig. 3 we would predict $S^{3/2} = (0.025\ \mathrm{A}^{-1})I_g$. This is consistent with the measured dependence on gradient but a significantly larger prefactor than seen experimentally. This difference may result from our assumption that the end of the crystal is flat. Surface-tension arguments alone would suggest a convex surface, extending upward furthest at $r = 0$, but it may well be faceted. There may also be an effective reduction in the radial extent of the mode due to nonuniformities in $H_d$ across the section (i.e., $\alpha_\infty$ may be larger than assumed).

In summary, we find that the model predicts behavior strikingly similar to that which is observed experimentally: notably, the correct qualitative dependence of the node structure on the magnitude and sense of the field gradient and on the position of the end of the crystal with respect to the NMR coil. In addition, we obtain the proper dependence on frequency near the turning point and would expect the behavior to deviate from a logarithmic dependence on frequency far from the turning point. Our explanation of the experiment suggests that in the region near $H_{\max}$ we are creating a helical transverse magnetization with a pitch of as little as a micrometer. This is sufficiently small that in more carefully controlled experiments it might be possible to study the effects of exchange and diffusional damping on these modes as a function of temperature and mode number. It is particularly interesting to study such phenomena in the high-field ordered phase, where it seems difficult to study spin propagation more directly. In addition, we stress that while the behavior we have presented results from a very special geometry, related nonlocal spin dynamics can be seen in many geometries in which a variation in field or sample cross section or magnetization lead to a local maximum in the field within the sample.

One of us (M.C.C.) wishes to acknowledge useful discussions with Barry Simon and Peter Weichman and was supported by the National Science Foundation through Grant No. DMR-84-12543.

[1]See, for example, D. D. Osheroff, H. Godfrin, and R. Ruel, Phys. Rev. Lett. **58**, 2458 (1987); D. D. Osheroff and R. C. Richardson, Phys. Rev. Lett. **54**, 1178 (1985).

[2]M. C. Cross and D. S. Fisher, Rev. Mod. Phys. **57**, 881 (1985).

[3]L. R. Walker, Phys. Rev. **105**, 390 (1957).

[4]R. I. Joseph and E. Schlömann, J. Appl. Phys. **32**, 1001 (1961), have considered the general case in cylinders.

[5]There are corrections to the slope $S$ coming from deviations from the WKB approximations but these are unimportant for $\Gamma/\alpha_\infty$ small. The form of the spectrum, however, is not changed in this limit.